ANNUAL REVIEWS

Annual Review of Control, Robotics, and Autonomous Systems

Microrobotics and Microorganisms: Biohybrid Autonomous Cellular Robots

Yunus Alapan,[1,*] Oncay Yasa,[1,*] Berk Yigit,[1] I. Ceren Yasa,[1] Pelin Erkoc,[1] and Metin Sitti[1,2]

[1]Physical Intelligence Department, Max Planck Institute for Intelligent Systems, 70569 Stuttgart, Germany; email: sitti@is.mpg.de

[2]School of Medicine and Department of Mechanical Engineering, Koç University, 34450 Istanbul, Turkey

Annu. Rev. Control Robot. Auton. Syst. 2019. 2:205–30

First published as a Review in Advance on December 3, 2018

The *Annual Review of Control, Robotics, and Autonomous Systems* is online at control.annualreviews.org

https://doi.org/10.1146/annurev-control-053018-023803

*These authors contributed equally to this article

Keywords

biohybrid microrobots, bacteria, neutrophils, artificial carriers, magnetic control, cargo delivery

Abstract

Biohybrid microrobots, composed of a living organism integrated with an artificial carrier, offer great advantages for the miniaturization of devices with onboard actuation, sensing, and control functionalities and can perform multiple tasks, including manipulation, cargo delivery, and targeting, at nano- and microscales. Over the past decade, various microorganisms and artificial carriers have been integrated to develop unique biohybrid microrobots that can swim or crawl inside the body, in order to overcome the challenges encountered by the current cargo delivery systems. Here, we first focus on the locomotion mechanisms of microorganisms at the microscale, crucial criteria for the selection of biohybrid microrobot components, and the integration of the selected artificial and biological components using various physical and chemical techniques. We then critically review biohybrid microrobots that have been designed and used to perform specific tasks in vivo. Finally, we discuss key challenges, including fabrication efficiency, swarm manipulation, in vivo imaging, and immunogenicity, that should be overcome before biohybrid microrobots transition to clinical use.

1. INTRODUCTION

Control over the microscopic world, at the size scale of individual cells, depends on the efficient miniaturization of functional machines that can operate at nano- and microscales (1, 2). The actuation, power, and sensing capabilities of microrobots have progressed at an incredible pace in the last decade, mainly due to advancements in fabrication techniques and new design paradigms (3, 4). The different types of microrobots include catalytic micromotors, bio-inspired microrobots, and biohybrid cellular microrobots (5). While catalytic micromotors rely on enzymatic reactions for propulsion, bio-inspired microrobots are powered mainly by global magnetic fields. Biohybrid microrobots, by contrast, take advantage of the inherently available onboard actuation and sensing mechanisms of motile microorganisms, such as bacteria and algae. Furthermore, through simple modifications to materials or surface chemistries, advanced functionalities such as drug transport, targeted cellular interactions, and heat generation can be further incorporated into microrobots.

Successful microrobotic applications in the human body require the incorporation of sensing, computational capability, and power for actuation. In contrast to their synthetic counterparts, microorganism-powered biohybrid microrobots can sense and respond to changes in their local environment, providing a higher level of autonomy. In addition, most microorganisms can achieve high propulsion speeds (tens of their body lengths per second) and interact with their targets at the same size scale (1–10 μm), which is also compatible with the smallest capillaries and interstitial spaces found in the human body. Such advantages make biohybrid cellular microrobots attractive candidates for medical applications, including targeted drug delivery.

Designing a biohybrid microrobot requires careful evaluation and selection of a motile microorganism, as well as additional artificial components for generating desired therapeutic effects. While selection of the microorganism affects mainly the propulsion and control characteristics of the microrobot, attached synthetic constructs govern the type of therapy, such as drug transport or hyperthermia. In addition, the compatibility of the microorganism and the synthetic construct in terms of integration efficiency and yield should be considered in order to achieve facile and high-throughput fabrication. In parallel, the safety of the microorganisms and materials used in synthetic constructs, including their degradability and immunogenicity, should be considered during the design process.

The objective of this article is to provide a comprehensive review of biohybrid microrobot design, fabrication, and control schemes and their potential medical applications for minimally invasive therapies (**Figure 1**). We focus on microorganisms, such as sperms, neutrophils, algae, and bacteria, that can be utilized to power biohybrid microrobots. First, we explain the locomotion modalities of the microorganisms in order to provide an understanding of motility and actuation in the microscopic world. Next, we critically review the desired properties of the artificial constructs and the approaches used to integrate them into the microorganisms. Finally, we describe the important biohybrid microrobot designs used in medical applications and discuss key challenges for improving the concept of the biohybrid microrobotics.

2. THE MOTILITY OF MICROORGANISMS

Motility at the micron scale refers to the autonomous motion of a microorganism via the coordinated organization and powering of its internal molecular motors through the harvesting of chemical energy from its local environment. The motility of microorganisms is vital for the successful continuation of life for both prokaryotes (such as bacteria for nutrient searching) and eukaryotes (such as mammalian cells for reproduction). There are various mechanisms of locomotion at the micron scale, but most mammalian cells use amoeboid movement to crawl over

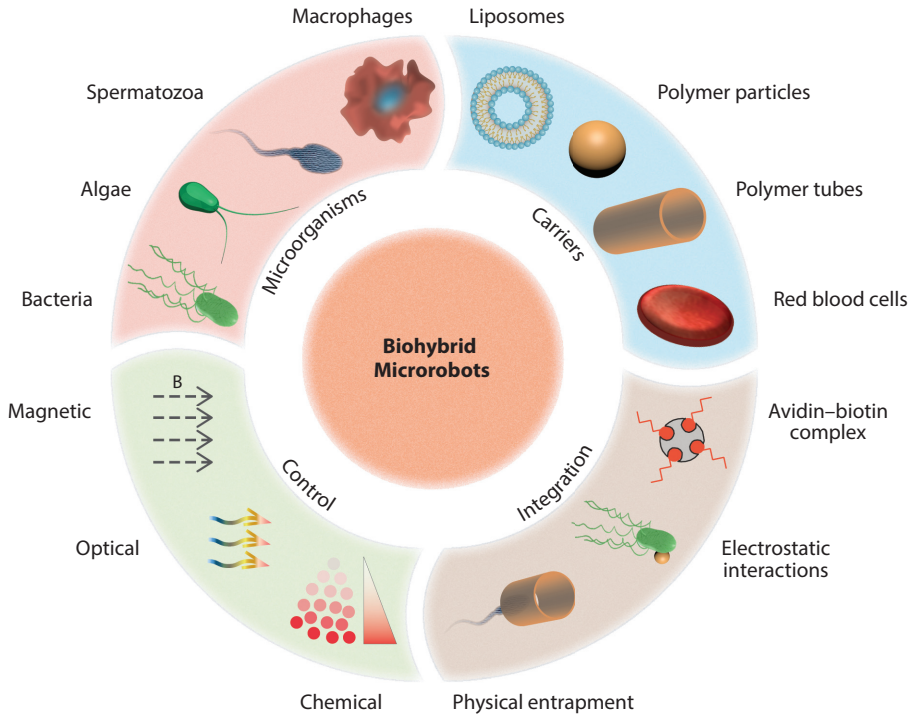

Figure 1

Design, fabrication, and control of biohybrid microrobots. Biohybrid microrobots are composed of a motile microorganism integrated with an artificial carrier and can be controlled using local chemical gradients, global magnetic fields, and light.

surfaces, and swimming of both eukaryotes and prokaryotes is facilitated by flexible surface appendages, including flagella and cilia. In this section, we briefly describe the amoeboid locomotion used by adherent mammalian cells and explain the swimming mechanisms employed by various microorganisms, along with their actuation in complex media.

2.1. Amoeboid Movement

Cell locomotion is a highly dynamic process and essential for fundamental biological activities, including embryonic development, wound healing, taxis, and immune response. Amoeboid movement is considered the most effective type of cell migration, mimicking the behavior of the amoeba *Dictyostelium discoideum* (6). Many mammalian cells, including leukocytes, lymphoma cells, and hematopoietic stem cells, migrate by amoeboid movement, which is driven by forces applied by their membrane protrusions to overcome the friction between the cell surface and the surrounding environment (7) (**Figure 2*a***). The actin cytoskeleton is the primary and essential coordinator of this process, transmitting the generated force to the substrate and recycling it when necessary (8, 9). In the first step of the movement, actin reorganization, filament bundling, and cross-linking in the form of filopodia and lamellipodia enable cells to change their elastic properties and increase the rigidity of the actin filaments to drive membrane extensions (10). Actin protrusions are formed in the cell's leading edge, which is determined by the type and gradient of the signal, and the membrane is propelled forward while new adhesion sites are generated for attachment to the

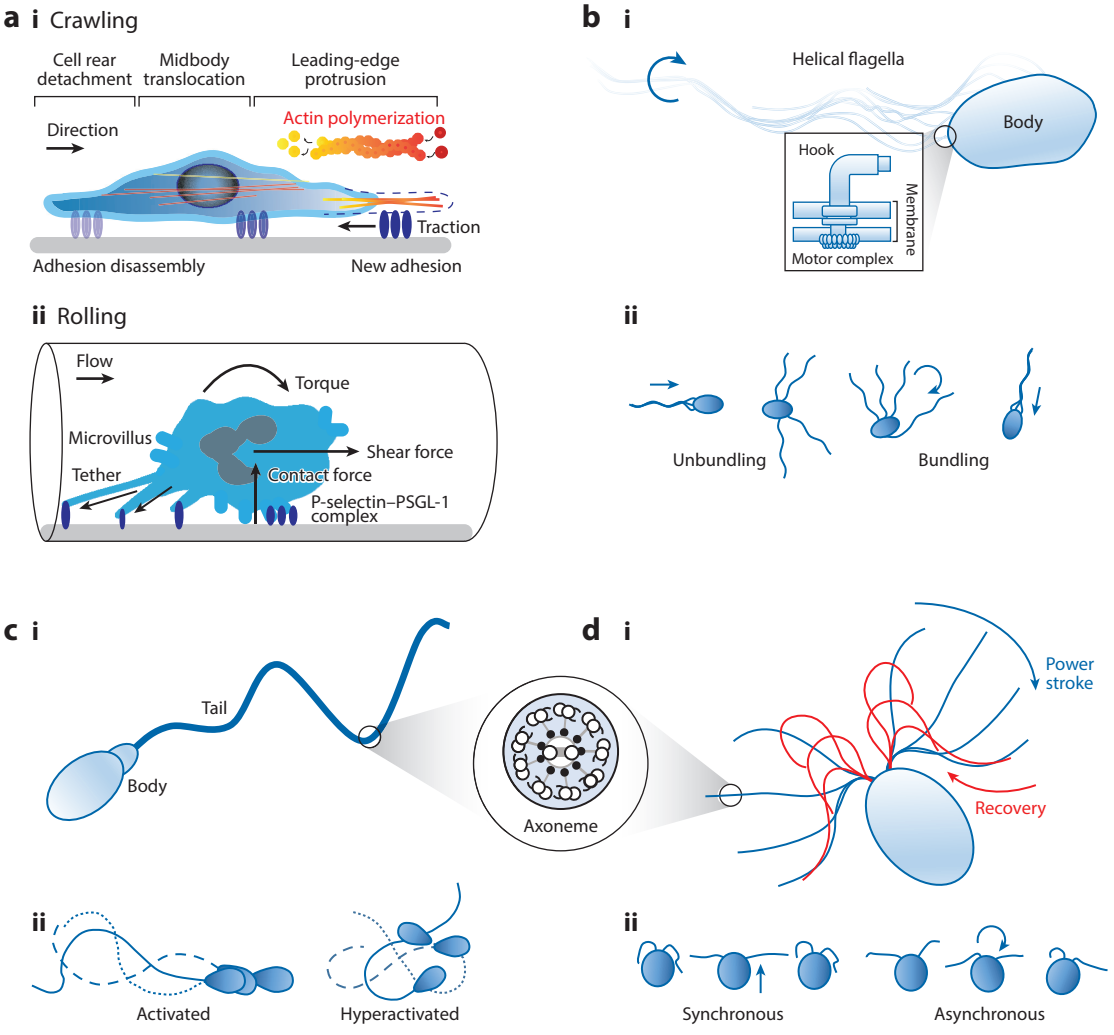

Figure 2

Schematic depiction of different mobility strategies used by microorganisms and cells. (*a*, *i*) Amoeboid movement of mammalian cells on a two-dimensional surface or endothelium. Cells extend a protrusion by actin polymerization in the direction of migration and form new adhesion sites on the leading edge. (*ii*) Rolling of the leukocytes on the endothelium during intraluminal migration. Forces acting on the cells include contact force, shear force, and torque created by blood flow, and tethering of the microvillus at the cell rear is shown. (*b*, *i*) Flagellated swimming of a peritrichous bacterium using corkscrew rotation. The inset shows the hook-basal body complex, including the flagellar motor. (*ii*) Run-and-tumble sequences mediated by bundling and unbundling of the flagella. (*c*, *i*) Flagellar swimming of spermatozoa using whip-like undulations of the active tail. The inset shows the cross-sectional structure of the eukaryotic flagella (axoneme), consisting of microtubules and motor dynein proteins that drive distributed actuation along the length of the eukaryotic flagella. (*ii*) Activated swimming mode of sperms near a surface where flagella undergo wave-like undulations for forward swimming (*left*) and sperms transitioning to hyperactivated mode, where they show a vigorous type of flagellar motion that leads to chaotic displacements in aqueous medium (*right*). (*d*, *i*) Biflagellated swimming of *Chlamydomonas reinhardtii*, in which flagella undergo an asymmetric beating cycle consisting of a power stroke (forward propulsion) followed by a recovery stroke. (*ii*) The two swimming modes that algae alternate between: synchronous beating of the flagella for forward propulsion (*left*) and asynchronous beating to change their orientations (*right*), akin to the run-and-tumble motion of bacteria.

substrate. A contractile force is then created by the acto-myosin network to pull the cell body forward in the direction of migration. Cells crawl by cyclically repeating these two main steps. The contractile force is generated through repetition of the three-step process of myosin motor protein binding, power stroke, and unbinding on actin filaments (11).

In addition to force generation, adhesion mechanics play an important role in the crawling behavior. Adhesion is reprocessed by emergence and disintegration from the substrate. For example, migration on the endothelial surface or in two-dimensional extracellular matrices requires integrin-dependent adhesion and adhesion forces, as well as the spatial distribution of the attachment sites, which determines the rate of translocation. However, leukocyte crawling in three dimensions both in vitro and in vivo is integrin independent and mediated only by cytoskeletal reorganization, shape changing, and squeezing through narrow regions (12). Similarly, amoeboid migration is different from collective or mesenchymal migration (i.e., smooth muscle cells and fibroblasts) in terms of lacking strong adhesive interactions and preserving tissue integrity (13). Neutrophils, for instance, can move at speeds of up to 30 μm/min with amoeboid migration by using protease-independent mechanisms to overcome matrix barriers, while fibroblasts move much more slowly (1 μm/min) due to the generation of strong adhesions, stable focal contacts with extracellular matrices, and proteolytic tissue remodeling. Leukocyte subtypes also differ in speed (lymphocytes can move at up to 25 μm/min, dendritic cells at up to 10 μm/min, and monocytes at up to 5 μm/ min) owing to differences in their myosin II activity and the deformability of their nuclei (6). Cells perform this active motion with high energy efficiency and execute their complex responses in a highly targeted manner due to their high sensing capacities (14).

Apart from amoeboid movement, leukocytes display rolling-arrhythmic tumbling on endothelial surfaces, which is mediated by the formation and dissociation of noncovalent bonding between P-selectin and P-selectin glycoprotein ligand-1 (PSGL-1) expressed in microvilli during intraluminal migration (15). Hydrodynamic shear force and torque created by the blood flow affect the bond kinetics and the dissociation time, and the increasing shear force results in increasing tethering force at the cell rear and contact force where the leukocyte contacts the endothelium, which enables new bond formation and resistance to high shear stress. When the bonds at the cell rear have too much stress, causing bond detachment, the cell undergoes rolling (16). As in crawling, as the cell rolls, new bonds are formed in the front part, and the old bonds start bearing the stress. Rolling is followed by slow rolling, arrest, crawling, and transmigration.

2.2. Swimming at the Microscale

Swimming is a highly efficient locomotion modality employed by many prokaryotic and eukaryotic microorganisms, enabling propulsion speeds on the order of tens of body lengths per second. The physics of swimming of microorganisms is fundamentally different from physics at the macroscale. At the microscale, fluidic forces imposed on a swimmer are dominated by viscous stresses over inertia. The Reynolds number is defined as $Re = \rho UL/\mu$, where ρ and μ are the fluid density and viscosity, respectively; U is the characteristic speed; and L is the characteristic length scale of the swimmer. The Reynolds number can be interpreted as the ratio of inertial to viscous forces on the body of a swimmer. For a bacterium like *Escherichia coli*, which has a typical body length of 2 μm and swims at typical speeds of approximately 30 μm/s in water, the Reynolds number would be on the order of 10^{-5}–10^{-4}. Therefore, in low-Reynolds-number regimes ($Re \ll 1$), flows generated by the microorganisms are governed by viscous stresses rather than the inertial effects that are prominent for swimmers at the macroscale. Fluid flows in low-Reynolds-number regimes are governed by the Stokes equations and boundary conditions imposed by the body

deformations of the swimmer and the surrounding geometries:

$$\mu \nabla^2 \mathbf{u} - \nabla p + \mathbf{f} = 0, \quad 1.$$

$$\nabla \cdot \mathbf{u} = 0, \quad 2.$$

where $\mathbf{u}$ is the velocity field, p is the pressure, and $\mathbf{f}$ is the volumetric forces imposed on the fluid by the swimmers and the boundaries. The Stokes equations are linear and have no time-dependent terms. Thus, a swimmer undergoing reciprocal motion would not be able to perform a net motion in Newtonian fluids, as demonstrated by Purcell (17) in his scallop theorem. In order to swim, microorganisms must perform nonreciprocal body deformations to generate drag-based thrust, using modalities such as the corkscrew motion of bacterial flagella, undulating flagellar waves of spermatozoa, and asymmetric beating of algal flagella.

2.2.1. Propulsion modalities. Flagellated bacteria rotate their flagella to generate propulsion. The bacterial flagellum is a passive polymeric organelle that is attached to the cell body via the hook-basal body complex and is rotated by the bacterial rotary motor, which is a true molecular engine that is capable of exerting torque on the flagella (18). Propulsion results from the rotation of the flagella, since chirality introduced by its helical geometry leads to conversion of its rotational motion into a translational thrust force (19). The number and position of the flagella vary across bacterial species: Monotrichous bacteria have a single flagellum, peritrichous bacteria have many flagella randomly distributed over their bodies, lophotrichous bacteria have multiple flagella gathered at one end of their bodies, and amphitrichous bacteria have one or multiple flagella at each end of their bodies. Bacteria commonly perform the so-called run-and-tumble motion, a sort of random walk, to explore their surroundings. In multiflagellated bacteria, such as *E. coli*, the separate run and tumble sequences are mediated by bundling and unbundling of the flagella (19, 20) (**Figure 2*b***). During the run phase, all flagella rotate counterclockwise, which leads to bundling. Bundling enables the bacterium to swim in a straight path. During tumbling, one or more bacterial motors change their rotational direction and thus the flagella unbundle, which causes the bacterium to change its orientation.

Spermatozoa are the quintessential eukaryotic swimmers that carry genetic material for reproduction. Like all eukaryotic unicellular swimmers, they use undulations of their flagella to generate thrust. Eukaryotic flagella are flexible and are actuated by an axoneme consisting of multiple structural microtubules and dynein motor complexes distributed along their length. The flagellum changes its curvature when microtubules on one side of the axoneme extend by sliding over each other via the action of dynein motors. Spermatozoa achieve propulsion by generating traveling wave-like undulations along their flagella. Spermatozoa are capable of swimming at high speeds (3–5 mm/min) and are able to survive in the female reproductive tract for extended periods of time (days) while maintaining their motility (21). The female reproductive tract presents a series of challenges for spermatozoa before they reach the ovum, including highly viscoelastic mucous barriers and the tortuous and narrow lumens of the fallopian tubes (22). Spermatozoa overcome these obstacles by displaying a variety of swimming modalities, including undulations; helical, hyperhelical, and hyperactivated movements; chiral ribbons; and slithering, depending on the geometrical, physiological, chemical, and rheological stimuli in their environment (22–24) (**Figure 2*c***).

Motile microscopic algae, such as *Chlamydomonas reinhardtii*, which are commonly found in freshwater and marine systems, constitute another class of eukaryotic swimmers. *C. reinhardtii* algae are biflagellated, and their two flagella are positioned in front of their bodies. Algal flagella

are structurally and functionally similar to sperm flagella but have a different beating pattern. For swimming, the flagella undergo a two-beat sequence of asymmetric deformations that resembles the breaststroke pattern in human swimming (25). During the power stroke, the flagellum stretches out and moves rapidly from the front to the sides of the algae; then, during the recovery stroke, the flagellum is bent (compacted) and moves slowly in the opposite direction (**Figure 2*d***). The stretched configuration is subjected to a larger hydrodynamic drag than the bent configuration, and the resulting asymmetry in drag between consecutive strokes enables net propulsion (19). *C. reinhardtii* algae beat their flagella in a synchronized fashion to swim in a straight path and can change their orientation by performing asynchronous beating (26, 27). By alternating between synchronous and asynchronous beating sequences, algae can randomize their trajectories, similarly to the run-and-tumble behavior of the bacteria (27).

2.2.2. Hydrodynamic interactions of swimmers with surfaces. Biological swimmers show a rich variety of behaviors when they are near boundaries. *E. coli* bacteria accumulate near walls and swim in circular trajectories with deterministic clockwise rotations due to the counterclockwise rotation of their flagella (28, 29). As such, they preferentially follow boundaries on their right side when they are swimming in channels, which can be used to guide them along desired directions at microchannel intersections (30). Spermatozoa also tend to accumulate over and follow boundaries (31, 32), which is thought to play a role in their guidance by the microarchitecture of the female reproductive tract (33, 34). The variety of behaviors shown by the microorganisms near boundaries are governed by swimmer-induced long-range flows and short-range ciliary interactions (32, 35–38). Understanding the interactions of swimmers with boundaries can enable the design of microdevice geometries that guide microrobots into desired organizations, for example, to control the direction of the motion in microchannels with ratcheting walls and guiding posts (32, 39), power microscopic gears and micromotors (40, 41), funnel swimmers, and generate directed colloidal transport through ratcheting geometries (42, 43).

2.2.3. Swimming in non-Newtonian fluids. The explanation of swimming mechanics above dealt with Newtonian fluids; however, many biological microorganisms live and move in complex media that exhibit non-Newtonian behavior, such as mucus, soil, and biofilms. In particular, almost all biological fluids, including synovial fluid, blood, mucus, and vitreous humor of the eye, display non-Newtonian material properties (44). Non-Newtonian behavior arises from interactions of the internal structure of complex media, which might consist of networks of polymeric chains, colloidal particles, and interstitial fluid (45). Non-Newtonian fluids exhibit shear-rate-dependent viscosity and elastic stresses that give fluid a restorative force, which can significantly influence the locomotion of biological swimmers. Non-Newtonian effects can significantly alter the mechanics of swimming. For instance, the presence of elastic forces or shear-rate-dependent viscosity renders the requirements of the scallop theorem obsolete in non-Newtonian media, and swimmers can generate net motion by reciprocal deformations (46, 47). The viscoelastic response of a fluid is generally measured by the Deborah number, $De = \lambda f$, where λ is the fluid relaxation time and f is the frequency of perturbations. The response of a fluid to perturbations varies from purely viscous when $De = 0$ to purely elastic as $De \to \infty$, which highlights that viscoelasticity is a frequency-dependent phenomenon. For a sperm cell beating its tail at a frequency range of 20–50 Hz in cervical mucus with a relaxation time of 1–10 s, the Deborah number can be estimated to be much greater than unity; therefore, elastic forces are thought to play a significant role in swimming dynamics (45).

Non-Newtonian media can significantly affect swimmer mobility depending on the propulsion modalities of the swimmers and the properties of the media. *E. coli* swimming speed decreases

with increasing polymer concentration (and, thus, viscosity) in Newtonian regimes (48, 49) but increases, to some extent, in certain polymeric solutions with long chains due to shear thinning of fluid around fast-rotating flagella (49) and elastic stresses (50). Spermatozoa (51) and *C. reinhardtii* (52) move more slowly in viscoelastic media. Furthermore, the gait behaviors of microorganisms are affected by the viscoelastic properties of the media. An increase in the viscosity of the suspending polymeric fluid caused *E. coli* to tumble less and swim straight due to an increase in flagellar bundling time (50, 53). It is widely known that spermatozoa enter a hyperactivated state inside fallopian tubes, where they perform a vigorous type of flagellar motion. Hyperactivation enhances sperm penetration through viscoelastic media and the zona pellucida of the egg, and cells that are unable to hyperactivate are incapable of fertilization (54, 55). *C. reinhardtii* algae change their gait patterns in viscoelastic fluids by beating their flagella faster and with smaller amplitudes, which reduces power consumption compared with their gait in Newtonian regimes, albeit with hindered mobility (52, 56).

3. SELECTION OF LIVING ENTITIES AND ARTIFICIAL CARRIERS

The fabrication of biohybrid microrobots requires a well-thought-out design approach since the desired functional output depends greatly on the performance of the selected microorganisms and artificial structures and their efficient integration. In this section, we systematically review various approaches that have been developed for selecting microorganisms and artificial carriers in biohybrid microrobot design.

3.1. Selection of Microorganisms

The selection of the microorganism to be used in a biohybrid microrobot design depends in large part on the desired medical application due to the varying physical, chemical, and biological environments and properties of different parts of the human body. For instance, the circulatory system includes both arteries with high flow rates (100–400 mm/s) and capillaries with extremely small diameters (<10 μm) (57), which requires a microorganism that is both strong enough to propel the microrobot against the arterial flow and small or soft enough to pass through the capillaries. Although a strain of magnetotactic bacteria, *Magnetospirillum magneticum*, can swim upstream in flow speeds of up to 600 μm/s (58), this bacterium would not be able to generate sufficient propulsion in arteries (59). Another size limitation for biohybrid microrobots is presented by mucosal barriers, which prevent transport of foreign pathogens and particles to the underlying epithelium in respiratory, gastrointestinal, and cervicovaginal tracts (60). The mucus layer, consisting of a polymer-based hydrogel, filters particles based on their size and interactions with the mucus components, meaning that any biohybrid microrobot that needs to penetrate the mucus layer must be smaller than the pore size and inert against mucus components. Another approach to penetrating the mucus layer may be the use of attenuated strains of enzymatically active bacteria (61) or synthetic enzyme-loaded structures (62) that can locally change the pH of the environment, which would result in a gel–sol transition of mucus and propulsion of the biohybrid microrobot.

In addition, body temperature may not be optimal for the motility of all microorganisms. While *E. coli* and *Salmonella typhimurium* can sustain and even increase their swimming speed at 37°C (63, 64), some strains of magnetotactic bacteria slow down with increasing temperatures, which limits their operation time in the body to 30–45 min (59). Similarly, the penetration depth of light through skin and tissues hinders the application of phototactic microorganisms, such as green algae, in deeper regions of the body. Furthermore, natural accumulation of microorganisms in specific locations of the human body due to their inherent taxis capability might be exploited for

targeted therapies. Bacterial species, including certain members of the *Salmonella*, *Bifidobacterium*, and *Escherichia* genera, can invade and colonize hypoxic regions of solid tumors owing to their taxis behavior (65, 66). Similarly, immune cells can autonomously recruit into pathological tissues using their intrinsic taxis mechanisms to search and defend the body.

Overall, several factors—including the propulsion strength, optimum motility conditions, taxis behaviors, safety concerns related to pathogenicity, interaction with surfaces, and propulsion in complex bodily fluids—should be critically investigated before the fabrication of biohybrid microrobots. Furthermore, technical advantages in fabrication, such as ease of cultivation and integration with artificial substrates, might play a crucial role in the selection of microorganisms in biohybrid microrobot design.

3.2. Selection of Artificial Carriers

Artificial substrates attached to microorganisms can provide additional capabilities to biohybrid microrobots, including magnetic steerability, drug encapsulation and release, and specific interactions with targeted cells and tissues. The properties of the artificial substrates depend greatly on the desired application of the microrobot. For example, drug loading and release require porous material selection, and encoding interactions with targeted cells necessitates a biochemically active surface. Regardless of the specific application, all artificial carriers need to enable the integration and viability of the microorganisms. A myriad of artificial carriers with different sizes, shapes, and materials have been developed and demonstrated in biohybrid microrobot fabrication, and here we describe the key features of these carriers, including size and shape, cargo loading and release, degradability, and deformability.

3.2.1. Size and shape. The size and shape of artificial components are crucial determinants of the propulsion and drug-loading performance of biohybrid microrobots. The size of the artificial component compared with the microorganisms used for actuation can be (*a*) larger, generally with a large number of microorganisms propelling the substrate; (*b*) approximately the same, with one or two microorganisms propelling the substrate; or (*c*) smaller, with a single microorganism carrying a large number of substrates on its surface or in the intracellular space. So far, studies have demonstrated the use of large numbers of attached bacteria to propel large (10–100 μm) synthetic substrates with shapes ranging from two-dimensional sheets to three-dimensional spheres and cubes (67–71). While using large numbers of microorganisms should simply generate greater propulsion forces, the uncontrolled orientation of the microorganisms results mostly in the cancellation of these forces, leading to translational speeds that are relatively similar to those for smaller substrates (67, 70). Furthermore, higher propulsion speeds were reported for biohybrid microrobots in which the substrate size was similar to or smaller than the actuating microorganism size, which can be attributed to a smaller drag on the microrobots and a smaller surface area not obstructing the flagella of the attached microorganisms (72, 73). On the other hand, the usage of smaller artificial substrates significantly lowers cargo-loading capacity since particle volume scales down with L^3 (where L is the isomorphic characteristic length scale), necessitating high-throughput fabrication of biohybrid microrobots to achieve an equivalent volume of cargo delivery. In addition, the increased directionality of biohybrid microrobots, even in the absence of external magnetic fields, can be achieved by using nonspherical particles or tubular structures (74–76). Similarly, circular substrates with ratchets (micromotors) can be used to generate rotational motion by bacteria integrated into top or side surfaces (40, 41, 67, 77, 78).

3.2.2. Cargo loading and release. Artificial substrates integrated with microorganisms are key components of biohybrid microrobots that can provide advanced functionalities, from magnetic steering to drug delivery, through molecules and particles loaded onto their surfaces or inner spaces. Cargo-loading capability depends in large part on the material composition of artificial substrates. Efficient cargo loading can be achieved by using porous materials, such as biological hydrogels, or empty vesicles, such as liposomes or cell ghosts. Loading of drug molecules, genes, photosensitizers, and antibiotics, including paclitaxel (79, 80), docetaxel (81), doxorubicin (82–84), mRNAs (85), indocyanine green (84), and ciprofloxacin (86), into a variety of artificial substrates, including nano- and microliposomes (79, 80), poly(lactic-*co*-glycolic) acid (PLGA) particles (81), mesoporous silica nanoparticles (83) and microtubes (86), red blood cell (RBC) ghosts (84), and polyelectrolyte multilayers (82), has been shown in microrobotic applications. While the propulsion of drug-loaded biohybrid microrobots was demonstrated for short periods, further investigations are needed to confirm the noninvasiveness of any potential drug toward the biological unit. In addition, the cargo, such as nanoparticles and drug molecules, can be directly loaded onto the microorganism membrane or into the intracellular space despite the risk of perturbed cellular functions (87–89). Furthermore, the release of the loaded cargo can be modulated by mechanisms that respond to a stimulus such as pH (82, 86), which can be advantageous in targeted disease sites with local biophysical and biochemical environments that are distinctly different from those of healthy tissues.

3.2.3. Interactions with biological units and target cells. Programming desired interactions of artificial carriers with biological units and targeted cells or tissues is crucial for the efficient propulsion and targeted delivery capabilities of biohybrid microrobots. Especially when the artificial carrier is larger than the microorganism, the effect of the number of bacteria on microrobot speed is not significant, unless the microorganism orientation and attachment site are controlled (70, 90). Several strategies, including the use of Janus particles with selectively functionalized and/or blocked hemispheres (90–94), liposomes with bioactive raft domains (70), metal-capped spherical particles (73), microtubes with bioactive internal surface area (76), and microfluidic laminar flow deposition (71), have been developed to achieve spatially controlled attachment of microorganisms. In addition, secondary interactions can be encoded on artificial substrates for selective targeting of specific cells or tissues, using antibodies or aptamers. Furthermore, the use of particles coated with cell membranes, such as the membranes of RBCs or white blood cells (WBCs), can enable interactions with specific cells or microorganisms due to the ligands and receptors that are inherently present on cell membranes (95, 96). WBC-membrane-coated particles would be particularly useful for targeting damaged vasculature and pathogens that would naturally bind to WBCs in the human body (97). However, combining such membrane-coated particles with biological propellers requires extra caution to avoid any unintended invasive interactions between the membrane ligands and the biological unit. Aside from patterning adhesive interactions, microorganisms can be guided to desired parts of synthetic substrates using physical guides, such as base ramps leading to microchambers of a motor (41).

3.2.4. Biocompatibility and biodegradability. Artificial carriers incorporated into biohybrid microrobot design should not elicit an inflammatory response or cause toxicity toward nontarget healthy cells. Therefore, the use of biocompatible materials, such as poly(ethylene glycol) (PEG) and PLGA, in the fabrication of artificial carriers is crucial in medical applications of biohybrid microrobots. Similarly, these carriers should also be nontoxic to propelling microorganisms to preserve vital functions, including motility and taxis behavior. In addition, artificial carriers in biohybrid microrobots should degrade in the body after the desired intervention without generating

any unintended or toxic by-products. Various materials have been used to fabricate biodegradable carriers in biohybrid microrobots, including emulsions (98), PEG (91), alginate (93), polycaprolactone (71), PLGA (81), and RBCs (84). Designing carriers that can degrade upon specific cues, such as a pH change or body enzymes, at the local environment of the targeted area can enable the release of drugs or other cargoes in a controlled way (99, 100).

3.2.5. Deformability. The deformability of synthetic carriers can be a crucial feature for biohybrid microrobots, especially when the carrier size is comparable to or larger than the propelling microorganism size. When navigating inside the body, biohybrid microrobots may need to go through confined spaces, depending on the route of administration and site of action, which necessitates the ability to deform and adapt to such environments without losing their integrity and functionality. For example, biohybrid microrobots targeting deep body locations through the circulatory system would need to pass through capillaries, which can be as small as few microns, and interstitial tissue space. In human physiology, both nonmobile RBCs and mobile WBCs are deformable, which allows them to passively or actively reach deep locations of the body. For microrobotic designs, liposomal constructs (98) and RBC ghosts (84) are inherently soft carriers, although RBC ghosts may be mechanically more stable for long-term operations. RBCs are nature's own carriers and have remarkable flexibility due to the loss of their nuclei through maturation, which allows them to travel through capillaries half their size without jamming (101–103). Alapan et al. (84) demonstrated the deformability of biohybrid microrobots composed of *E. coli* and cargo-loaded RBCs by manually injecting microrobots through microchannels smaller than the microrobots. They also demonstrated active deformation of the RBC carriers through confined spaces using only bacterial propulsion, which proves that when the carrier is soft enough, propulsion of microorganisms might be more than sufficient to propel and squeeze a microrobot through tight spaces.

4. FABRICATION STRATEGIES AND CONTROL SCHEMES FOR BIOHYBRID MICROROBOTS

4.1. Biohybrid Microrobot Fabrication

The fabrication of biohybrid microrobots requires integrating the two main components—the microorganisms and the artificial carriers—using various physical and chemical techniques (104, 105). The process of selecting the microorganisms and the artificial carriers based on the envisioned application limits the fabrication strategies to certain techniques due to possible unforeseen alterations of physical and/or chemical properties of the components. For example, the use of chemical cross-linking reactions, such as those of carbodiimide cross-linkers, for biohybrid microrobot fabrication alters the cell membrane proteins of the microorganisms in an uncontrolled way. Consequently, different populations of microorganisms might lose their intrinsic properties, including motility, taxis, and targeting, which eventually could lead to uncontrolled fabrication of different biohybrid microrobots with unknown physical and chemical properties. Therefore, it is crucial to take into account the feasibility of fabrication strategies while selecting the microorganisms and the artificial carriers for particular medical applications. In this section, we focus on the four main integration methodologies that have generally been utilized to fabricate biohybrid microrobots: noncovalent interactions, covalent interactions, physical entrapment, and internalization.

4.1.1. Noncovalent interactions. Taking advantage of noncovalent interactions for biohybrid microrobot fabrication is straightforward. The noninvasive nature of these interactions is important to fabricate biohybrid microrobots with well-preserved surface properties. The different uses of noncovalent interactions could also be classified into different categories according to their strength and complexity. An example of the simplest way to fabricate biohybrid microrobots using noncovalent interactions is the case of polystyrene particles and *Serratia marcescens*. The electrostatic interactions between negatively charged polystyrene particles and naturally positively charged *S. marcescens* are sufficient to create biohybrid microrobots (67, 106). Physical techniques, such as plasma treatment and physisorption, can then be used to focus the position of the noncovalent interactions on certain locations of the artificial carriers for enhanced propulsion (90, 107). In addition to charge, in the case of some bacteria species, such as *E. coli*, alteration of the artificial carriers' surface properties, such as softness, is also important to fabricate biohybrid microrobots using noncovalent interactions and to enhance the fabrication efficiency. Park et al. (82) demonstrated that modifying polystyrene particles using oppositely charged polyelectrolytes can provide a soft interface for bacterial adhesion and enable noninvasive, highly efficient fabrication of biohybrid microrobots. Additionally, the surfaces of the microorganisms can be modified with biotin-conjugated antibodies through antibody–antigen interactions to noninvasively fabricate biohybrid microrobots (108). Finally, bioengineered strains of microorganisms can be utilized to fabricate biohybrid microrobots through noninvasive modifications of the bacteria and the artificial carrier membranes. Alapan et al. (84) utilized a bioengineered strain of *E. coli* to fabricate biohybrid microrobots using a biotin–avidin–biotin complex. Another technique is to integrate biotin into the membranes of bacterial and artificial carriers through peptide interactions and antibody binding, respectively, and then sandwich avidin with the biotin-containing segments (**Figure 3*a***).

4.1.2. Covalent interactions. As an alternative to noninvasive fabrication techniques, the covalent modification of microorganisms with molecules and the direct covalent attachment of artificial carriers to microorganisms have been used to integrate microorganisms with artificial carriers. If it is not straightforward to create adhesion between the microorganisms and the artificial carriers through noncovalent interactions, then chemical reactions, such as carbodiimide and click chemistry, can be utilized to modify the microorganisms, the artificial carriers, or both in order to achieve proper integration. Various chemical reactions have been used to attach artificial carriers of different sizes to bacteria (72, 98), algae (109), and lymphocytes (110). Covalent interactions provide stable adhesion between the actuators and the artificial carriers and can be further utilized for the controlled release of the cargo at desired positions (109) (**Figure 3*b***). However, the effects of chemical reactions on the microorganisms in terms of their motility, cell membranes, and genetic material should be addressed for biohybrid microrobots that will be used in a medical application.

4.1.3. Physical entrapment. For artificial carriers with certain geometries (e.g., hollow tubes), microorganisms can be physically entrapped by the carrier moieties (**Figure 3*c***). This strategy has been used mainly to fabricate biohybrid microrobots powered by sperms (75, 111–113) and was initially demonstrated using dynamic trapping that took advantage of the increase in sperms' flagellar oscillation amplitude toward their distal ends. It was subsequently demonstrated that biochemical modifications of the interiors of the microtubes (e.g., using fibronectin) can further enhance the binding of sperms to the microtubes after physical entrapment. Stanton et al. (76, 86) also recently adapted a physical entrapment strategy for bacterial biohybrid microrobots. The authors modified the interiors of the microtubes with bacteria-attractant polydopamine molecules, thereby easing the fabrication and formation of the biohybrid microrobots by favoring the

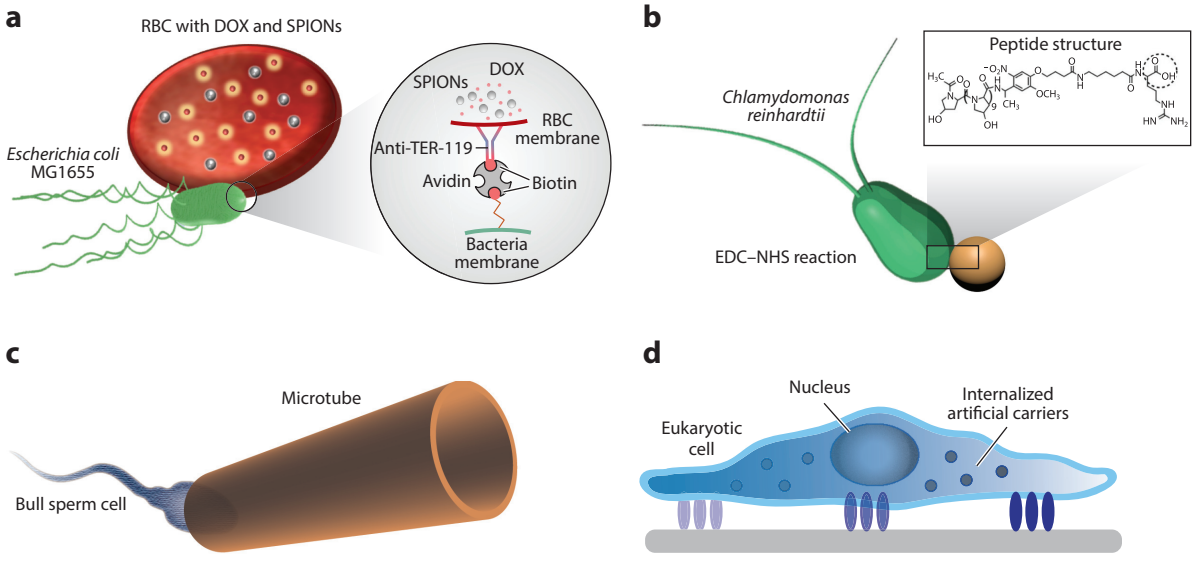

Figure 3

The four strategies that have been primarily used in the fabrication of biohybrid microrobots: (*a*) noncovalent interactions, (*b*) covalent interactions, (*c*) physical entrapment, and (*d*) internalization. Abbreviations: DOX, doxorubicin; EDC, *N*-ethyl-*N*′-[3-(dimethylamino) propyl]carbodiimide; NHS, *N*-hydroxysuccinimide; RBC, red blood cell; SPION, super-paramagnetic iron oxide nanoparticle. Panel *a* adapted from Reference 84 with permission. Panel *b* adapted from Reference 109; copyright 2005 National Academy of Sciences.

attachment of the bacteria inside the microtubes. Like every method, physical entrapment has advantages and disadvantages. The advantages are that it does not affect any cellular activity or motility and provides highly directional swimming. The disadvantage is that biohybrid microrobot formation is limited to the action of the microorganisms, which means that entrapment of the microorganisms in the tubes occurs stochastically, even if the artificial carriers can be modified with chemoattractant molecules.

4.1.4. Internalization. Internalization is utilized mainly to fabricate biohybrid microrobots from surface walkers, such as macrophages and neutrophils (114) (**Figure 3*d***). The first study of photothermal therapy that used tumor-associated macrophages successfully reported the development of a gold nanoshell–monocyte hybrid therapeutic strategy using phagocytosis of nanoshells by the cells (115). Other studies have demonstrated the internalization of colloidal particles (116), drug molecules (83, 89, 117), and magnetic iron-oxide particles (81) by T cells, neutrophils, and sperms. When this strategy is used to fabricate biohybrid microrobots for medical applications, the main concern is the possible effects of internalized molecules and particles on the viability, behavior, and genetic material of the cells.

4.2. Biohybrid Microrobot Control Schemes

Control of microrobot motion is critical for biohybrid microrobot design and successful task completion. Control over motion can be achieved by using inherent characteristics of either the microorganisms or the artificial carriers attached to them. Moreover, control stimuli can be

generated externally by an operator (e.g., using magnetic or electric fields) or received from the local environment (e.g., using nutrients, temperature, or pH). For instance, bacterial microrobots can be designed that swim toward gradients of chemoattractants or can be controlled through the alignment of magnetic cargo in the direction of an externally applied magnetic field. While relying on the sensing capabilities of the microorganisms provides autonomy and self-guiding in most cases, taxis response time to environmental changes can be slow (up to tens of seconds). Guiding microrobot motility using external fields, by contrast, allows rapid control but requires imaging and feedback loop control strategies, which can be challenging for in vivo operations. The optimal control method (or combination of methods) for microrobot motility must be included in the design process and chosen according to the specific application.

4.2.1. Magnetic control. Magnetic fields can be used to generate a magnetic torque on the biohybrid microrobot, which results in the alignment of the propulsion direction with the magnetic field direction. To generate magnetic torque on biohybrid microrobots, either the biological component or the attached artificial carrier should possess magnetic properties. Some microorganisms, such as MTB-1, inherently possess magnetic properties due to intracellular production of magnetic crystals, which allows them to align their direction with Earth's magnetic field (58, 72, 118). Moreover, naturally nonmagnetic microorganisms, such as macrophages or *Tetrahymena pyriformis*, can be magnetically engineered by induced production of intracellular magnetic crystals or internalization of magnetic iron particles that are seeded in the growth environment (81, 119). Alternatively, magnetic steering of the biohybrid microrobots can be achieved by attaching microorganisms to magnetic constructs of different shapes and sizes, which enables facile magnetic control of microorganisms that lack innate magnetic properties (76, 82, 84, 89, 120).

One of the most attractive features of magnetic fields is that they can safely penetrate deeply into the human body, which makes them ideal for actuation of biohybrid microrobots. Strong magnetic fields can be generated using either electromagnets or permanent magnets. While electromagnets can rapidly and precisely generate homogeneous magnetic fields upon the application of electrical currents, the heat generated by those same currents is a major limitation. Permanent magnets do not heat but require precise positioning and motion to generate the desired fields. Different magnetic actuation approaches might be more favorable in specific applications depending on the route of administration and the distance from the site of administration to the site of action.

Various magnetic control schemes have been integrated into different biohybrid microrobots to obtain steering functionalities. Han et al. (81) manipulated microrobots for active targeting through magnetic intervention using macrophages that internalized docetaxel-loaded PLGA nanoparticles and magnetite (Fe_3O_4) nanoparticles. They showed both the magnetic recruitment of cell aggregates toward a tumor spheroid in vitro with a speed of up to 50 μm/s and the positive effect of actively delivered docetaxel on reducing tumor cell viability. In a related study, Nguyen et al. (80) used macrophages with a magnetization saturation value of 8.15 emu/g to carry paclitaxel-encapsulated 150-nm magnetic liposomes to breast and colorectal cancer models in vitro, using electromagnetic actuation and chemotaxis of cells and achieving an average speed of 10.48 μm/s. They demonstrated tumor targeting and the induced therapeutic effect of the paclitaxel in CT-26 mouse colon carcinoma cells and 4T1 mouse breast cancer cells. However, free magnetic liposomes with encapsulated drug showed a greater amount of release compared with macrophage-engulfed counterparts. Furthermore, Yan et al. (121) reported a basic, low-cost mass-production method to create microswimmers using a helical microalga species, *Spirulina platensis*, as a biotemplate. They immersed the microalgae in magnetite suspensions to induce crystallization on the organism surface and thereby enable magnetic steering. The same group recently reported that these biohybrid magnetic robots display intrinsic fluorescence, magnetic resonance signals,

natural degradability, and appropriate cytocompatibility; monitored the microswimmer navigation in real time; and tracked a swarm of microswimmers inside a rodent stomach by magnetic resonance imaging (MRI) in vivo (122). In addition, Yasa et al. (123) presented magnetic control of *C. reinhardtii*–powered biohybrid microrobots and tracked the three-dimensional motion of the microrobots under a uniform magnetic field. Finally, Magdanz et al. (75, 124) demonstrated the guidance of single spermatozoa by catching them in rolled-up ferromagnetic microtubes and remotely controlling their direction using an external field. In 2016, the same group extended the previous work on spermbots by using magnetic microhelices to transport an immotile sperm cell to the oocyte with the aim of fertilization (125). Around the same time, this group also used a thermoresponsive polymer, poly(*N*-isopropylacrylamide) (PNIPAM), to fabricate a dynamic microtube for remote-controlled release of single sperm cells (113).

4.2.2. Chemical control. Chemical control of biohybrid microrobots relies on the intrinsic ability of microorganisms to sense chemical gradients in their local environments, which is governed by diffusion. The directional motility of the biohybrid microrobots was shown within microfluidic devices in the presence of different chemoattractants, including L-aspartate (69, 92, 126), L-serine (127), casamino acid (128), and α-methyl-DL-aspartate (82), and chemorepellents, such as $NiSO_4$ (92). Zhuang et al. (129) also demonstrated taxis of biohybrid microrobots in the presence of pH gradients, with the microrobots moving toward the optimal pH of the bacteria. In addition, several studies have analytically modeled and simulated the motion and chemotaxis of bacterial microrobots, actuated by *S. marcescens*, *S. typhimurium*, or *E. coli* (130–133). An attractive aspect of chemical control is the availability of a wide variety of chemical signals released locally by targeted cells or tissues, which can induce taxis behavior in different microorganisms. For example, biohybrid microrobots driven by neutrophils and macrophages were able to migrate toward chemoattractants generated by *E. coli* (83) and tumor cell lysate (80), respectively. Similarly, Park et al. (134) demonstrated the chemotactic motility of *S. typhimurium*–driven microrobots toward tumor cell lysates and spheroids in a microfluidic setup, as well as the accumulation of microrobots in tumors in a CT-26 tumor mouse model. Additionally, *E. coli* and *S. marcescens* can sense temporal changes in the concentration of chemical attractants (e.g., L-serine) and repellents (e.g., $NiCl_2$), and suppress their tumbling rate accordingly, switching from a random walk behavior to a biased random walk (127, 135).

Taxis-based chemical control can provide flexibility in design, but due to the large variety of attractants and repellents specific to different microorganisms, the large degree of stochasticity and low temporal resolution prevent straightforward and rapid steering of biohybrid microrobots. In addition, the formation of chemical gradients and their strength are limited by the diffusion and concentration of chemicals at the source, which hinders long-range chemotactic motility. Therefore, for in vivo applications, chemical control should ideally be coupled with a long-range, uniform control method, such as magnetic steering, that can first guide microrobots to the close proximity of target cells or tissues, after which chemotactic motility can provide further local guidance.

4.2.3. Optical control. Optical control of biohybrid microrobots can be in the form of steering (when phototactic microorganisms are used as actuators) or on/off control (for nonphototactic bacteria). Optical control can provide localized, parallel, and wavelength-specific control of biohybrid microrobots. Weibel et al. (109) showed that the direction of algal microrobots can be repeatedly changed upon application of LED light (500-nm wavelength) from opposite directions. Steager et al. (68) achieved on/off control of SU-8 microstructures (50 μm) powered by swarms of *S. marcescens* by using exposure to ultraviolet light, which stops the bacterial motility

within 5 s. Furthermore, Vizsnyiczai et al. (41) showed optical control of the speed of micromotors driven by a genetically engineered strain of *E. coli*, where the bacteria expressed a light-driven proton pump that allows the swimming speed to be tuned by changes in light intensity. Even though optical control is attractive due to the fast and specific response of phototactic microorganisms, the penetration limit of light is a major challenge for its use in vivo. In addition, long exposure to ultraviolet light is not feasible since it can damage both microorganisms and targeted cells or tissues.

4.2.4. Other control schemes. Electric fields can be used to control biohybrid microrobot motion through the galvanotaxis of microorganisms, which is directional propulsion in response to an electric field (136), although this method is limited to microfluidic applications. The selection of electrodes, as well as the magnitude and timescale of the applied electric potential, is critical to limit changes in media temperature and pH and biochemical damage to cells. Other taxis behaviors, such as thermotaxis and aerotaxis, can also be used to control the motion of biohybrid microrobots. Felfoul et al. (118) used aerotaxis in a study that demonstrated the accumulation of liposomes attached to *Magnetococcus marinus* strain MC-1 bacteria in hypoxic regions of HCT116 colorectal xenografts. Finally, Wu et al. (137) used ultrasound to control the actuation of magnetic nanoparticle–loaded RBCs and enable on/off control over their motion.

5. BIOHYBRID MICROROBOTS FOR MEDICINE

Biohybrid microrobots have the potential to revolutionize minimally invasive therapies, but their medical applications are still in the early stages, because of both the insufficient resolution and the acquisition speed of current imaging techniques and cellular complications caused by host immune responses to many microorganisms (138). In this section, we examine the disease models and routes of administration demonstrated by studies that have tested biohybrid microrobots in vivo.

In 2007, Akin et al. (139) performed the first in vivo study using biohybrid microrobots (**Figure 4*a***). They tested microrobot accumulation inside mouse organs after intraperitoneal injection of *Listeria monocytogenes*–based biohybrid microrobots. They fabricated the microrobots by attaching streptavidin-coated polystyrene nanoparticles to biotinylated antibody–modified bacterial cell membranes and then modifying the nanoparticles using biotinylated GFP plasmids. In vivo, the biohybrid microrobots effectively delivered their nucleic acid–based cargoes and eventually transfected the cells, as shown by functional protein expression observed with bioluminescence imaging 3 days after the treatment of the mice.

In 2013, Park et al. (134) developed biohybrid microrobots that integrated bioengineered attenuated *S. typhimurium* bacteria, which display biotin on their outer membrane proteins, with streptavidin-coated fluorescent microparticles. They tested microrobot accumulation inside tumor regions by using a CT-26 tumor mouse model. In vivo, they formed the tumors by subcutaneously injecting CT-26 cells; when the tumors had reached a critical volume, they systemically injected the biohybrid microrobots through the tail veins of the mice. Three days after the injection, they captured bioluminescence and near-infrared images of both the animals (in vivo) and extracted tumors (ex vivo) and demonstrated the accumulation of the biohybrid microrobots, but not the free microparticles, inside the tumor regions.

In 2016, Felfoul et al. (118) presented targeting of tumor hypoxic regions by using biohybrid microrobots actuated with magnetotactic bacteria (**Figure 4*b***). They fabricated the biohybrid microrobots by covalently binding drug-loaded nanoliposomes onto bacterial cell membranes and used the intrinsic magnetotaxis and aerotaxis mechanisms of the bacteria to target hypoxic regions

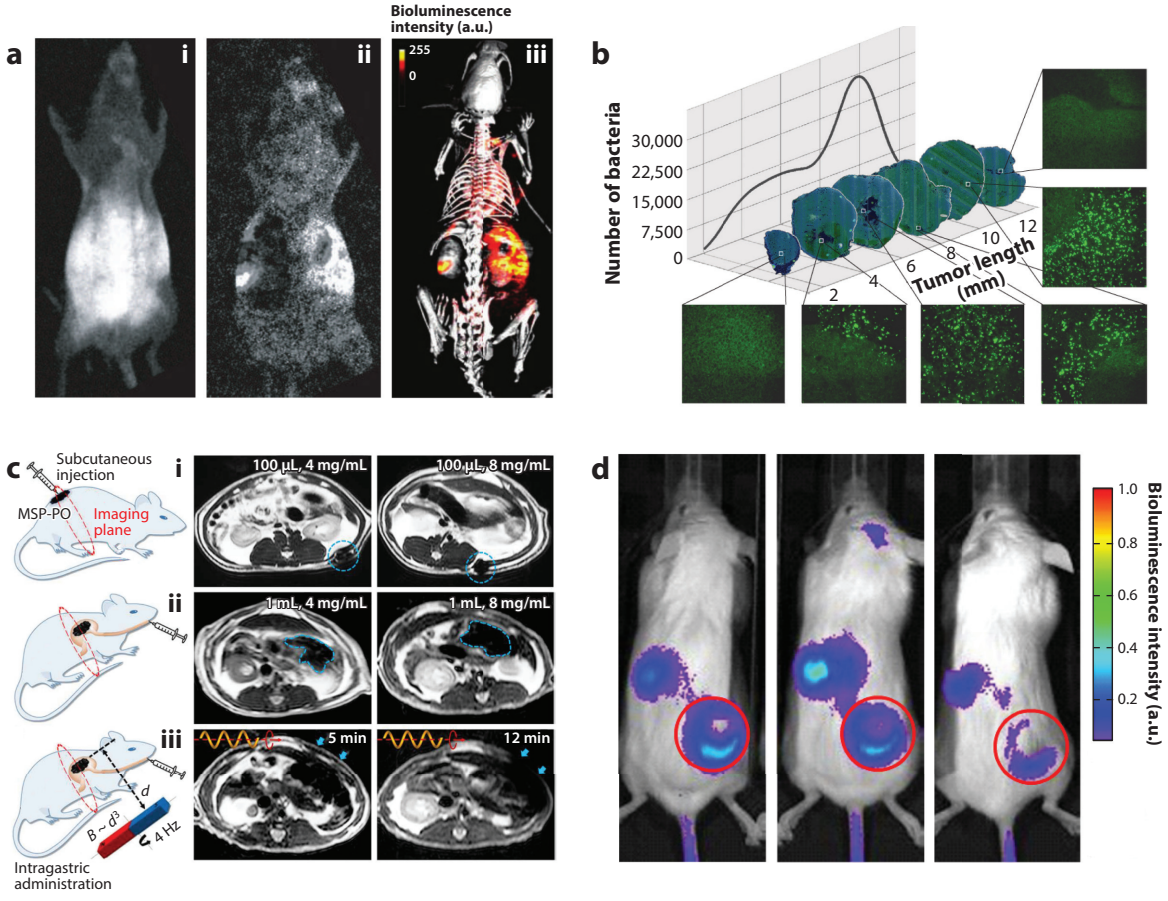

Figure 4

Biohybrid microrobots for medicine. (*a*) Characterization of in vivo protein expression 3 days after biohybrid microrobot injection into a mouse, using a bioluminescence imaging technique for (*i*) short and (*ii*) long (35 min) photon collection and integration periods, along with (*iii*) the anatomical location of the bioluminescence. (*b*) Transverse tumor sections after magnetic targeting of biohybrid microrobots. The images show a good distribution of biohybrid microrobots throughout the tumor. (*c*) Magnetic resonance imaging of biohybrid microrobot swarms inside subcutaneous tissue and stomach in the (*i*,*ii*) absence and (*iii*) presence of a magnetic field. Abbreviation, MSP-PO, magnetic *Spirulina platensis* in peanut oil solution. (*d*) Bioluminescent images of T cell biodistribution. T cells were retrovirally modified to express firefly luciferase and then loaded in the presence of gold colloids for 24 h. The cells were subsequently injected intravenously into mice bearing subcutaneous xenografted tumors. The images show the T cell localization at the tumor site (*red circle*) and within the spleen 48 h after injection. Panels *a*–*c* reproduced from References 139, 118, and 122, respectively, with permission. Panel *d* reproduced from Reference 116 under the Creative Commons Attribution 2.0 Generic license (**https://creativecommons.org/licenses/by/2.0**).

of solid tumors. The study used beige mice with severe combined immunodeficiency and utilized an external magnetic field to direct the biohybrid microrobots toward the interior of HCT116 tumor xenografts after the peritumoral injection. The results showed the penetration and accumulation of up to 55% of the biohybrid microrobots in the hypoxic regions of the tumors due to the intrinsic properties of the microrobots' biological actuators.

In 2017, Xie et al. (88) utilized a probiotic strain of *E. coli* (*E. coli* Nissle 1917) to deliver anticancer drug molecules to tumor environments. They created the biohybrid microrobots by conjugating doxorubicin onto bacterial cell membranes through acid-labile linkers of *cis*-aconitic

anhydride. The chosen conjugation method was utilized for acid-responsive release of the drug molecules in the tumor environment. The authors injected the fabricated biohybrid microrobots into mice with 4T1 tumors and investigated their accumulation inside the tumor environment after 3 h and 3 days of injections. The results demonstrated effective tumor growth inhibition, apoptosis of the tumor cells, and prolonged survival of the treated animals. Eventually, the biohybrid microrobots were eliminated from the animals' bodies with an antimicrobial treatment, which demonstrated the safety of using biohybrid microrobots for cancer therapy to some extent.

Beyond bacteria, biohybrid microrobots composed of microalgae, macrophages, T cells, or neutrophils have also been utilized in vivo for medical imaging and cancer therapy. In 2017, Yan et al. (122) demonstrated in vivo use of biohybrid microrobots composed of microalgae for imaging-guided therapy (**Figure 4*c***). They utilized the microalgae as templates to fabricate the biohybrid microrobots and an alternating magnetic field for the actuation of the whole system. Importantly, this study revealed that microalgae could be utilized in medical applications for fluorescence imaging and selective elimination of cancer cells.

As eukaryotic cells, macrophages, T cells, and neutrophils have also been utilized to generate precisely regulated robotic systems that act as Trojan horses, carrying therapeutic agents to targeted locations in vivo. The tumor-tropic migration behavior of monocytes can be exploited to develop biohybrid microrobots that can infiltrate tumor tissue when combined with a cargo unit. Such a strategy must ensure that its cargo does not have any harmful effects on the living host or carrier until delivery is completed. In 2011, Kennedy et al. (116) presented tumor-specific homing of human T cells loaded with gold colloids in a human tumor xenograft mouse model (**Figure 4*d***). This biohybrid approach enhanced the efficacy of nanoparticle-mediated photothermal therapy through an altered distribution of the cargo in the tumor environment compared with the free administration of gold colloids. Basel et al. (140) used monocytes and macrophages to carry magnetic nanoparticles for a magnetic field–induced hyperthermia-based cancer treatment in vivo. As an alternative to cargo uptake, Stephan et al. (110) demonstrated the stable chemical conjugation of drug carrier submicron particles to the surfaces of T lymphocytes without any interference with intrinsic cell functions. They attached 300-nm drug-loaded particles to cell surfaces with a density of 100 nanoparticles/cell through maleimide–thiol coupling followed by PEGylation to quench the residual reactive groups. The nanoparticle-drug-decorated T cells showed enhanced performance on accumulating cargo in antigen-presenting tumor tissue by transmigrating the endothelial barrier in a mouse tumor model.

Similar drug-carrying systems have been developed that utilize neutrophils. In one recent study, Xue et al. (117) used neutrophils to design a neutrophil-based drug carrier that inhibits the recurrence of a malignant glioma. They used simple co-incubation to load the neutrophils with cationic liposomes encapsulated with the anticancer drug paclitaxel, and tested the cytotoxicity of the agents in vitro in a blood–brain barrier model and in vivo in a glioma resection mouse model. In both conditions, drug-carrying neutrophil migration was inflammation directed and not controlled wirelessly. Nevertheless, the results demonstrated that neutrophil-based delivery and sustained release of the drugs from liposomes increased the survival rates in vivo and slowed the tumor growth, although it did not inhibit growth completely.

Overall, various administration routes have been chosen in studies that have investigated mainly the tumor-targeting capabilities of biohybrid microrobots actuated by a natural swimmer. Immunogenicity and in vivo real-time monitoring of these biohybrid microrobots are the main concerns that limit their in vivo application to certain body locations, and these challenges should be overcome to enable a better clinical transition. Additionally, leukocyte-based hybrid delivery systems depend on the natural migration of cells to hypoxic tumor tissues or released chemokines and lack active control. Their off-target migration to other tissues and possible side effects have

been poorly investigated and are unclear. Finally, these biohybrid microrobots usually move slowly, which diminishes their efficiency and leads to long treatment periods if they are intravenously administered rather than injected directly into the tumor. Many key challenges remain that need to be addressed in detail before these biohybrid microrobots can be used safely and efficiently in clinical applications.

6. KEY CHALLENGES AND FUTURE PERSPECTIVES

In the last decade, advanced fabrication and integration techniques have fueled the development of biohybrid microrobots with ever-increasing functionalities and niche applications. These tiny robots have demonstrated autonomous propulsion, durable and efficient cargo transportation, navigation using local chemical gradients or global magnetic fields, and on-demand drug release and self-termination by exploiting the inherent actuation and sensing mechanisms of the microorganisms and efficient loading of the artificial carriers. However, most of the biohybrid microrobots that have been developed for medical applications are still in their infancy, with many major challenges to overcome before they can translate to the clinic (141, 142). Here, we highlight some of the most pressing issues related to the use of biohybrid microrobots in the body.

6.1. Fabrication Efficiency and Throughput

One of the key challenges in the practical use of biohybrid microrobots is a lack of facile, reliable, and high-throughput culture, fabrication, and integration techniques that can ensure high-performance motility and functionality. Although the self-assembly techniques used so far allow high-throughput fabrication, the performance and efficiency of each microrobot can vary significantly. Moreover, although many different functionalities for biohybrid microrobots have been individually demonstrated, ensuring the reliable and sustainable combination of these functionalities might be challenging. For example, loading of magnetic nanoparticles will decrease the volume of drug that can be loaded in a carrier, and loading of some drugs may affect the motility and sensing of propelling microorganisms. In addition, the fabrication process produces not only biohybrid microrobots but also large numbers of free-swimming microorganisms and free-floating synthetic carriers. Therefore, biohybrid microrobots should be filtered from free units using noninvasive means, such as magnetic manipulation, without affecting their performance.

6.2. Swarm Manipulation

Advanced functionalities of various biohybrid microrobots have been demonstrated in isolated single units. However, the ability of a single microrobot to generate the desired therapeutic outcome in a target tissue or organ is limited, and successful real-world clinical applications will therefore require the collective motion and coordination of large numbers of biohybrid microrobots. Although the motility and global control of biohybrid swarms have been demonstrated, interactions between neighboring units and swarm coordination have not been investigated or engineered. Engineering swarm manipulation and passive guidance using physical cues will be especially critical for operating large numbers of biohybrid microrobots in complex and challenging in vivo conditions, where autonomy might dominate external control with the currently limited imaging modalities.

6.3. Imaging

Real-time tracking and localization of biohybrid microrobots are critical for feedback and external control. For successful clinical applications of biohybrid microrobots, current imaging techniques, including radiology, ultrasound, infrared, and MRI, should be improved in terms of their resolution and sensitivity, so that they can image single objects at the size of an individual cell in real time (143). Recently, efforts have been made to track swarms of biohybrid microrobots in vivo in various body locations by combining different techniques, such as MRI and fluorescence-based imaging. Due to the limited penetration depth of light, Yan et al. (122) utilized fluorescence-based imaging to track microrobots in subcutaneous tissue and intraperitoneal cavities and MRI to track them in deep body locations. Vilela et al. (144) used positron emission tomography in combination with computed tomography to track catalytic microrobots in a tubular phantom, demonstrating that this technique could be used to monitor biohybrid microrobots in vivo. As the functionality and control of biohybrid microrobots continue to improve, the sensitivity and resolution of imaging techniques should also improve for proper medical applications and use in clinics.

6.4. Propulsion in Biological Environments

Understanding how microorganisms interact with biological environments is crucial for the design and engineering of biohybrid microrobots for medical applications. In contrast to simple in vitro environments, where most biohybrid microrobots have been tested so far, in vivo environments present several challenges, including the complex rheology of biological fluids, the suspension of cells, the extracellular matrix with adhesive proteins, and biological barriers, such as the mucosa that lines respiratory and gastrointestinal tracts. Therefore, initial testing of future biohybrid microrobots should be performed in physiologically relevant in vitro conditions, recapitulating flow conditions, rheological properties, cellular composition, and structural morphology. Recent advances in microfluidic models and organ-on-a-chip systems might be ideal candidates for initial testing and optimization before small-animal experiments.

6.5. Safety and Immune Reactions

The immunogenicity of microorganisms is one of the major challenges related to using biohybrid microrobots in the body, since most of them are phagocytosed by innate immune cells, including macrophages and neutrophils. Biohybrid microrobots targeting disease sites with lower or suppressed immune reactions, such as the gastrointestinal system, might minimize immunogenicity concerns. On the other hand, the use of attenuated bacteria strains could provide a safer alternative for operations in different parts of the human body (105). Alternative approaches may include the use of less pathogenic microorganisms (e.g., *C. reinhardtii*) and the use of native cells of the body, including erythrocytes, macrophages, and sperms, which could circumvent some of the safety issues. For the development of biohybrid microrobots for in vivo operations, assessment of the safety risks and pharmacokinetics, including biodistribution, toxicity, retention, and biocompatibility, are of the utmost importance.

Another challenge for in vivo applications is how to remove or neutralize biohybrid microrobots after they have completed their task or in case of an emergency intervention. While the use of genetically engineered microorganisms with kill switches presents a promising way to deactivate biohybrid microrobots (145), performing the laborious and time-consuming development of such switches for every microorganism is not currently feasible. Instead, a fast and reliable alternative termination switch can be created by loading biohybrid microrobots with

photosensitizers or magnetic nanoparticles, which can be triggered using near-infrared light or alternating magnetic fields to generate sufficient heat for on-demand deactivation of biohybrid microrobots.

Overall, the last decade has seen a rapid increase in the development and applications of biohybrid microrobots. The use of biohybrid microrobots in medicine still presents many challenges, some of which are common to all microrobots and others of which are unique to certain designs, and there is no single recipe for developing the ideal biohybrid microrobot, since the required performance and functionality are highly dependent on the specific application. Therefore, the performance and functionality of biohybrid microrobots should be tailored and optimized for specific applications, which requires need-driven design in close collaboration with medical researchers. Such an approach would significantly enhance and accelerate the translation of biohybrid microrobots for medical use.

DISCLOSURE STATEMENT

The authors are not aware of any affiliations, memberships, funding, or financial holdings that might be perceived as affecting the objectivity of this review.

ACKNOWLEDGMENTS

This work is funded by the Max Planck Society. Y.A. thanks the Alexander von Humboldt Foundation for the Humboldt Postdoctoral Research Fellowship.

LITERATURE CITED

1. Sitti M. 2009. Miniature devices: voyage of the microrobots. *Nature* 458:1121–22
2. Sitti M. 2018. Miniature soft robots—road to the clinic. *Nat. Rev. Mater.* 3:74–75
3. Sitti M, Ceylan H, Hu W, Giltinan J, Turan M, et al. 2015. Biomedical applications of untethered mobile milli/microrobots. *Proc. IEEE* 103:205–24
4. Ricotti L, Trimmer B, Feinberg AW, Raman R, Parker KK, et al. 2017. Biohybrid actuators for robotics: a review of devices actuated by living cells. *Sci. Robot.* 2:eaaq0495
5. Sitti M. 2017. *Mobile Microrobotics*. Cambridge, MA: MIT Press
6. Friedl P, Weigelin B. 2008. Interstitial leukocyte migration and immune function. *Nat. Immunol.* 9:960–69
7. Bershadsky AD, Kozlov MM. 2011. Crawling cell locomotion revisited. *PNAS* 108:20275–76
8. Pollard TD, Cooper JA. 2009. Actin, a central player in cell shape and movement. *Science* 326:1208–12
9. Kruse K. 2016. Cell crawling driven by spontaneous actin polymerization waves. In *Physical Models of Cell Motility*, ed. IS Aranson, pp. 69–93. Cham, Switz.: Springer
10. Ananthakrishnan R, Ehrlicher A. 2007. The forces behind cell movement. *Int. J. Biol. Sci.* 3:303–17
11. Alberts B, Johnson A, Lewis J, Raff M, Roberts K, Walter P. 2002. *Molecular Biology of the Cell*. New York: Garland Sci.
12. Lammermann T, Bader BL, Monkley SJ, Worbs T, Wedlich-Soldner R, et al. 2008. Rapid leukocyte migration by integrin-independent flowing and squeezing. *Nature* 453:51–55
13. Friedl P. 2004. Prespecification and plasticity: shifting mechanisms of cell migration. *Curr. Opin. Cell Biol.* 16:14–23
14. Fischbach MA, Bluestone JA, Lim WA. 2013. Cell-based therapeutics: the next pillar of medicine. *Sci. Transl. Med.* 5:179ps7
15. Nourshargh S, Alon R. 2014. Leukocyte migration into inflamed tissues. *Immunity* 41:694–707
16. Sundd P, Pospieszalska MK, Cheung LS, Konstantopoulos K, Ley K. 2011. Biomechanics of leukocyte rolling. *Biorheology* 48:1–35

17. Purcell EM. 1977. Life at low Reynolds number. *Am. J. Phys.* 45:3–11
18. Lowe G, Meister M, Berg HC. 1987. Rapid rotation of flagellar bundles in swimming bacteria. *Nature* 325:637–40
19. Lauga E, Powers TR. 2009. The hydrodynamics of swimming microorganisms. *Rep. Prog. Phys.* 72:096601
20. Brennen C, Winet H. 1977. Fluid mechanics of propulsion by cilia and flagella. *Annu. Rev. Fluid Mech.* 9:339–98
21. Suarez SS, Pacey AA. 2006. Sperm transport in the female reproductive tract. *Hum. Reprod. Update* 12:23–37
22. Suarez SS. 2016. Mammalian sperm interactions with the female reproductive tract. *Cell Tissue Res.* 363:185–194
23. Eisenbach M, Giojalas LC. 2006. Sperm guidance in mammals – an unpaved road to the egg. *Nat. Rev. Mol. Cell Biol.* 7:276–85
24. Nosrati R, Driouchi A, Yip CM, Sinton D. 2015. Two-dimensional slither swimming of sperm within a micrometre of a surface. *Nat. Commun.* 6:8703
25. Rüffer U, Nultsch W. 1985. High-speed cinematographic analysis of the movement of *Chlamydomonas*. *Cell Motil.* 5:251–63
26. Rüffer U, Nultsch W. 1987. Comparison of the beating of cis- and trans-flagella of *Chlamydomonas* cells held on micropipettes. *Cell Motil. Cytoskelet.* 7:87–93
27. Polin M, Tuval I, Drescher K, Gollub JP, Goldstein RE. 2009. *Chlamydomonas* swims with two "gears" in a eukaryotic version of run-and-tumble locomotion. *Science* 325:487–90
28. Frymier PD, Ford RM, Berg HC, Cummings PT. 1995. Three-dimensional tracking of motile bacteria near a solid planar surface. *PNAS* 92:6195–99
29. Lauga E, DiLuzio WR, Whitesides GM, Stone HA. 2006. Swimming in circles: motion of bacteria near solid boundaries. *Biophys. J.* 90:400–12
30. DiLuzio WR, Turner L, Mayer M, Garstecki P, Weibel DB, et al. 2005. *Escherichia coli* swim on the right-hand side. *Nature* 435:1271–74
31. Rothschild. 1963. Non-random distribution of bull spermatozoa in a drop of sperm suspension. *Nature* 198:1221–22
32. Denissenko P, Kantsler V, Smith DJ, Kirkman-Brown J. 2012. Human spermatozoa migration in microchannels reveals boundary-following navigation. *PNAS* 109:8007–10
33. Tung C-K, Ardon F, Fiore AG, Suarez SS, Wu M. 2014. Cooperative roles of biological flow and surface topography in guiding sperm migration revealed by a microfluidic model. *Lab Chip* 14:1348–56
34. Veronika M, Britta K, Samuel S, Schmidt OG. 2015. Sperm dynamics in tubular confinement. *Small* 11:781–85
35. Berke AP, Turner L, Berg HC, Lauga E. 2008. Hydrodynamic attraction of swimming microorganisms by surfaces. *Phys. Rev. Lett.* 101:038102
36. Drescher K, Dunkel J, Cisneros LH, Ganguly S, Goldstein RE. 2011. Fluid dynamics and noise in bacterial cell–cell and cell–surface scattering. *PNAS* 108:10940–45
37. Kantsler V, Dunkel J, Polin M, Goldstein RE. 2013. Ciliary contact interactions dominate surface scattering of swimming eukaryotes. *PNAS* 110:1187–92
38. Lushi E, Kantsler V, Goldstein RE. 2017. Scattering of biflagellate microswimmers from surfaces. *Phys. Rev. E* 96:023102
39. Sipos O, Nagy K, Di Leonardo R, Galajda P. 2015. Hydrodynamic trapping of swimming bacteria by convex walls. *Phys. Rev. Lett.* 114:258104
40. Di Leonardo R, Angelani L, Dell'Arciprete D, Ruocco G, Iebba V, et al. 2010. Bacterial ratchet motors. *PNAS* 107:9541–45
41. Vizsnyiczai G, Frangipane G, Maggi C, Saglimbeni F, Bianchi S, Di Leonardo R. 2017. Light controlled 3D micromotors powered by bacteria. *Nat. Commun.* 8:15974
42. Galajda P, Keymer J, Chaikin P, Austin R. 2007. A wall of funnels concentrates swimming bacteria. *J. Bacteriol.* 189:8704–7

43. Koumakis N, Lepore A, Maggi C, Di Leonardo R. 2013. Targeted delivery of colloids by swimming bacteria. *Nat. Commun.* 4:2588
44. Fung YC. 1981. *Biomechanics: Mechanical Properties of Living Tissues*. New York: Springer
45. Sznitman J, Arratia PE. 2015. In *Complex Fluids in Biological Systems: Experiment, Theory, and Computation*, ed. SE Spagnolie, pp. 245–81. New York: Springer
46. Keim NC, Garcia M, Arratia PE. 2012. Fluid elasticity can enable propulsion at low Reynolds number. *Phys. Fluids* 24:081703
47. Qiu T, Lee T-C, Mark AG, Morozov KI, Münster R, et al. 2014. Swimming by reciprocal motion at low Reynolds number. *Nat. Commun.* 5:5119
48. Berg HC, Turner L. 1979. Movement of microorganisms in viscous environments. *Nature* 278:349–51
49. Martinez VA, Schwarz-Linek J, Reufer M, Wilson LG, Morozov AN, Poon WCK. 2014. Flagellated bacterial motility in polymer solutions. *PNAS* 111:17771–76
50. Patteson AE, Gopinath A, Goulian M, Arratia PE. 2015. Running and tumbling with *E. coli* in polymeric solutions. *Sci. Rep.* 5:15761
51. Tung C-K, Hu L, Fiore AG, Ardon F, Hickman DG, et al. 2015. Microgrooves and fluid flows provide preferential passageways for sperm over pathogen *Tritrichomonas foetus. PNAS* 112:5431–36
52. Qin B, Gopinath A, Yang J, Gollub JP, Arratia PE. 2015. Flagellar kinematics and swimming of algal cells in viscoelastic fluids. *Sci. Rep.* 5:9190
53. Qu Z, Temel FZ, Henderikx R, Breuer KS. 2018. Changes in the flagellar bundling time account for variations in swimming behavior of flagellated bacteria in viscous media. *PNAS* 115:1707–12
54. Suarez SS, Dai X. 1992. Hyperactivation enhances mouse sperm capacity for penetrating viscoelastic media. *Biol. Reprod.* 46:686–91
55. Quill TA, Sugden SA, Rossi KL, Doolittle LK, Hammer RE, Garbers DL. 2003. Hyperactivated sperm motility driven by CatSper2 is required for fertilization. *PNAS* 100:14869–74
56. Li C, Qin B, Gopinath A, Arratia PE, Thomases B, Guy RD. 2017. Flagellar swimming in viscoelastic fluids: role of fluid elastic stress revealed by simulations based on experimental data. *J. R. Soc. Interface* 14:20170289
57. Nelson BJ, Kaliakatsos IK, Abbott JJ. 2010. Microrobots for minimally invasive medicine. *Annu. Rev. Biomed. Eng.* 12:55–85
58. Rismani Yazdi S, Nosrati R, Stevens CA, Vogel D, Davies PL, Escobedo C. 2018. Magnetotaxis enables magnetotactic bacteria to navigate in flow. *Small* 14:1870019
59. Felfoul O, Martel S. 2013. Assessment of navigation control strategy for magnetotactic bacteria in microchannel: toward targeting solid tumors. *Biomed. Microdevices* 15:1015–24
60. Lieleg O, Vladescu I, Ribbeck K. 2010. Characterization of particle translocation through mucin hydrogels. *Biophys. J.* 98:1782–89
61. Celli JP, Turner BS, Afdhal NH, Keates S, Ghiran I, et al. 2009. *Helicobacter pylori* moves through mucus by reducing mucin viscoelasticity. *PNAS* 106:14321–26
62. Walker D, Käsdorf BT, Jeong H-H, Lieleg O, Fischer P. 2015. Enzymatically active biomimetic micropropellers for the penetration of mucin gels. *Sci. Adv.* 1:e1500501
63. Maeda K, Imae Y, Shioi JI, Oosawa F. 1976. Effect of temperature on motility and chemotaxis of *Escherichia coli*. *J. Bacteriol.* 127:1039–46
64. Magariyama Y, Sugiyama S, Kudo S. 2001. Bacterial swimming speed and rotation rate of bundled flagella. *FEMS Microbiol. Lett.* 199:125–29
65. Forbes NS. 2010. Engineering the perfect (bacterial) cancer therapy. *Nat. Rev. Cancer* 10:785–94
66. Kocijancic D, Felgner S, Frahm M, Komoll R-M, Iljazovic A, et al. 2016. Therapy of solid tumors using probiotic Symbioflor-2–restraints and potential. *Oncotarget* 7:22605
67. Darnton N, Turner L, Breuer K, Berg HC. 2004. Moving fluid with bacterial carpets. *Biophys. J.* 86:1863–70
68. Steager E, Kim C, Patel J, Bith S, Naik C, et al. 2007. Control of microfabricated structures powered by flagellated bacteria using phototaxis. *Appl. Phys. Lett.* 90:263901
69. Kim D, Liu A, Diller E, Sitti M. 2012. Chemotactic steering of bacteria propelled microbeads. *Biomed. Microdevices* 14:1009–17

70. Kojima M, Zhang Z, Nakajima M, Fukuda T. 2012. High efficiency motility of bacteria-driven liposome with raft domain binding method. *Biomed. Microdevices* 14:1027–32
71. Huh K, Oh D, Son SY, Yoo HJ, Song B, et al. 2016. Laminar flow assisted anisotropic bacteria absorption for chemotaxis delivery of bacteria-attached microparticle. *Micro Nano Syst. Lett.* 4:1
72. Taherkhani S, Mohammadi M, Daoud J, Martel S, Tabrizian M. 2014. Covalent binding of nanoliposomes to the surface of magnetotactic bacteria for the synthesis of self-propelled therapeutic agents. *ACS Nano* 8:5049–60
73. Stanton MM, Juliane S, Xing M, Albert ML, Samuel S. 2016. Biohybrid Janus motors driven by *Escherichia coli*. *Adv. Mater. Interfaces* 3:1500505
74. Sahari A, Headen D, Behkam B. 2012. Effect of body shape on the motile behavior of bacteria-powered swimming microrobots (BacteriaBots). *Biomed. Microdevices* 14:999–1007
75. Magdanz V, Sanchez S, Schmidt OG. 2013. Development of a sperm-flagella driven micro-bio-robot. *Adv. Mater.* 25:6581–88
76. Stanton MM, Park BW, Miguel-Lopez A, Ma X, Sitti M, Sanchez S. 2017. Biohybrid microtube swimmers driven by single captured bacteria. *Small* 13:1603679
77. Hiratsuka Y, Miyata M, Tada T, Uyeda TQP. 2006. A microrotary motor powered by bacteria. *PNAS* 103:13618–23
78. Sokolov A, Apodaca MM, Grzybowski BA, Aranson IS. 2010. Swimming bacteria power microscopic gears. *PNAS* 107:969–74
79. Nguyen VD, Han JW, Choi YJ, Cho S, Zheng S, et al. 2016. Active tumor-therapeutic liposomal bacteriobot combining a drug (paclitaxel)-encapsulated liposome with targeting bacteria (*Salmonella Typhimurium*). *Sens. Actuators B* 224:217–24
80. Nguyen VD, Han JW, Go G, Zhen J, Zheng S, et al. 2017. Feasibility study of dual-targeting paclitaxel-loaded magnetic liposomes using electromagnetic actuation and macrophages. *Sens. Actuators B* 240:1226–36
81. Han J, Zhen J, Nguyen VD, Go G, Choi Y, et al. 2016. Hybrid-actuating macrophage-based microrobots for active cancer therapy. *Sci. Rep.* 6:28717
82. Park BW, Zhuang J, Yasa O, Sitti M. 2017. Multifunctional bacteria-driven microswimmers for targeted active drug delivery. *ACS Nano* 11:8910–23
83. Shao J, Xuan M, Zhang H, Lin X, Wu Z, He Q. 2017. Chemotaxis-guided hybrid neutrophil micromotors for targeted drug transport. *Angew. Chem. Int. Ed. Engl.* 56:12935–39
84. Alapan Y, Yasa O, Schauer O, Giltinan J, Tabak AF, et al. 2018. Soft erythrocyte-based bacterial microswimmers for cargo delivery. *Sci. Robot.* 3:eaar4423
85. Geerts N, McGrath J, Stronk JN, Vanderlick TK, Huszar G. 2014. Spermatozoa as a transport system of large unilamellar lipid vesicles into the oocyte. *Reprod. Biomed. Online* 28:451–61
86. Stanton MM, Park BW, Vilela D, Bente K, Faivre D, et al. 2017. Magnetotactic bacteria powered biohybrids target *E. coli* biofilms. *ACS Nano* 11:9968–78
87. Luo C-H, Huang C-T, Su C-H, Yeh C-S. 2016. Bacteria-mediated hypoxia-specific delivery of nanoparticles for tumors imaging and therapy. *Nano Lett.* 16:3493–99
88. Xie S, Zhao L, Song X, Tang M, Mo C, Li X. 2017. Doxorubicin-conjugated *Escherichia coli* Nissle 1917 swimmers to achieve tumor targeting and responsive drug release. *J. Control. Release* 268:390–99
89. Xu H, Medina-Sanchez M, Magdanz V, Schwarz L, Hebenstreit F, Schmidt OG. 2018. Sperm-hybrid micromotor for targeted drug delivery. *ACS Nano* 12:327–37
90. Behkam B, Sitti M. 2008. Effect of quantity and configuration of attached bacteria on bacterial propulsion of microbeads. *Appl. Phys. Lett.* 93:223901
91. Cho S, Park SJ, Ko SY, Park J-O, Park S. 2012. Development of bacteria-based microrobot using biocompatible poly(ethylene glycol). *Biomed. Microdevices* 14:1019–25
92. Park D, Park SJ, Cho S, Lee Y, Lee YK, et al. 2014. Motility analysis of bacteria-based microrobot (bacteriobot) using chemical gradient microchamber. *Biotechnol. Bioeng.* 111:134–43
93. Donghai L, Hyunchul C, Sunghoon C, Semi J, Zhen J, et al. 2015. A hybrid actuated microrobot using an electromagnetic field and flagellated bacteria for tumor-targeting therapy. *Biotechnol. Bioeng.* 112:1623–31

94. Vikram SA, Metin S. 2016. Patterned and specific attachment of bacteria on biohybrid bacteria-driven microswimmers. *Adv. Healthc. Mater.* 5:2325–31
95. Hu C-MJ, Fang RH, Wang K-C, Luk BT, Thamphiwatana S, et al. 2015. Nanoparticle biointerfacing by platelet membrane cloaking. *Nature* 526:118–21
96. Esteban-Fernández de Ávila B, Angsantikul P, Ramírez-Herrera DE, Soto F, Teymourian H, et al. 2018. Hybrid biomembrane–functionalized nanorobots for concurrent removal of pathogenic bacteria and toxins. *Sci. Robot.* 3:eaat0485
97. Esteban-Fernandez de Avila B, Gao W, Karshalev E, Zhang L, Wang J. 2018. Cell-like micromotors. *Acc. Chem. Res.* 51:1901–10
98. Singh A, Hosseinidoust Z, Park B-W, Yasa O, Sitti M. 2017. Microemulsion-based soft bacteria-driven microswimmers for active cargo delivery. *ACS Nano* 11:9759–69
99. Ceylan H, Yasa IC, Yasa O, Tabak AF, Giltinan J, Sitti M. 2018. 3D-printed biodegradable microswimmer for drug delivery and targeted cell labeling. bioRxiv 379024. **https://doi.org/10.1101/379024**
100. Bozuyuk U, Yasa O, Yasa IC, Ceylan H, Kizilel S, Sitti M. 2018. Light-triggered drug release from 3D-printed magnetic chitosan microswimmers. *ACS Nano* 12:9617–25
101. Alapan Y, Little JA, Gurkan UA. 2014. Heterogeneous red blood cell adhesion and deformability in sickle cell disease. *Sci. Rep.* 4:7173
102. Alapan Y, Fraiwan A, Kucukal E, Hasan MN, Ung R, et al. 2016. Emerging point-of-care technologies for sickle cell disease screening and monitoring. *Expert Rev. Med. Devices* 13:1073–93
103. Alapan Y, Kim C, Adhikari A, Gray KE, Gurkan-Cavusoglu E, et al. 2016. Sickle cell disease biochip: a functional red blood cell adhesion assay for monitoring sickle cell disease. *Transl. Res.* 173:74–91
104. Carlsen RW, Sitti M. 2014. Bio-hybrid cell-based actuators for microsystems. *Small* 10:3831–51
105. Hosseinidoust Z, Mostaghaci B, Yasa O, Park BW, Singh AV, Sitti M. 2016. Bioengineered and biohybrid bacteria-based systems for drug delivery. *Adv. Drug Deliv. Rev.* 106:27–44
106. Behkam B, Sitti M. 2007. Bacterial flagella-based propulsion and on/off motion control of microscale objects. *Appl. Phys. Lett.* 90:023902
107. Park SJ, Bae H, Kim J, Lim B, Park J, Park S. 2010. Motility enhancement of bacteria actuated microstructures using selective bacteria adhesion. *Lab Chip* 10:1706–11
108. Mostaghaci B, Yasa O, Zhuang J, Sitti M. 2017. Bioadhesive bacterial microswimmers for targeted drug delivery in the urinary and gastrointestinal tracts. *Adv. Sci.* 4:1700058
109. Weibel DB, Garstecki P, Ryan D, DiLuzio WR, Mayer M, et al. 2005. Microoxen: microorganisms to move microscale loads. *PNAS* 102:11963–67
110. Stephan MT, Moon JJ, Um SH, Bershteyn A, Irvine DJ. 2010. Therapeutic cell engineering with surface-conjugated synthetic nanoparticles. *Nat. Med.* 16:1035
111. Khalil ISM, Magdanz V, Sanchez S, Schmidt OG, Misra S. 2014. Biocompatible, accurate, and fully autonomous: a sperm-driven micro-bio-robot. *J. Micro-Bio Robot.* 9:79–86
112. Magdanz V, Medina-Sanchez M, Chen Y, Guix M, Schmidt OG. 2015. How to improve spermbot performance. *Adv. Funct. Mater.* 25:2763–70
113. Magdanz V, Guix M, Hebenstreit F, Schmidt OG. 2016. Dynamic polymeric microtubes for the remote-controlled capture, guidance, and release of sperm cells. *Adv. Mater.* 28:4084–89
114. Chen C, Chang X, Angsantikul P, Li J, Esteban-Fernández de Ávila B, et al. 2018. Chemotactic guidance of synthetic organic/inorganic payloads functionalized sperm micromotors. *Adv. Biosyst.* 2:1700160
115. Choi M-R, Stanton-Maxey KJ, Stanley JK, Levin CS, Bardhan R, et al. 2007. A cellular Trojan Horse for delivery of therapeutic nanoparticles into tumors. *Nano Lett.* 7:3759–65
116. Kennedy LC, Bear AS, Young JK, Lewinski NA, Kim J, et al. 2011. T cells enhance gold nanoparticle delivery to tumors in vivo. *Nanoscale Res. Lett.* 6:283
117. Xue J, Zhao Z, Zhang L, Xue L, Shen S, et al. 2017. Neutrophil-mediated anticancer drug delivery for suppression of postoperative malignant glioma recurrence. *Nat. Nanotechnol.* 12:692–700
118. Felfoul O, Mohammadi M, Taherkhani S, de Lanauze D, Xu YZ, et al. 2016. Magneto-aerotactic bacteria deliver drug-containing nanoliposomes to tumour hypoxic regions. *Nat. Nanotechnol.* 11:941–47
119. Kim DH, Cheang UK, Kőhidai L, Byun D, Kim MJ. 2010. Artificial magnetotactic motion control of *Tetrahymena pyriformis* using ferromagnetic nanoparticles: a tool for fabrication of microbiorobots. *Appl. Phys. Lett.* 97:173702

120. Carlsen RW, Edwards MR, Zhuang J, Pacoret C, Sitti M. 2014. Magnetic steering control of multicellular bio-hybrid microswimmers. *Lab Chip* 14:3850–59
121. Yan X, Zhou Q, Yu J, Xu T, Deng Y, et al. 2015. Magnetite nanostructured porous hollow helical microswimmers for targeted delivery. *Adv. Funct. Mater.* 25:5333–42
122. Yan X, Zhou Q, Vincent M, Deng Y, Yu J, et al. 2017. Multifunctional biohybrid magnetite microrobots for imaging-guided therapy. *Sci. Robot.* 2:eaaq1155
123. Yasa O, Erkoc P, Alapan Y, Sitti M. 2018. Microalga-powered microswimmers toward active cargo delivery. *Adv. Mater.* 30:1804130
124. Magdanz V, Medina-Sanchez M, Schwarz L, Xu HF, Elgeti J, Schmidt OG. 2017. Spermatozoa as functional components of robotic microswimmers. *Adv. Mater.* 29:1606301
125. Medina-Sanchez M, Schwarz L, Meyer AK, Hebenstreit F, Schmidt OG. 2016. Cellular cargo delivery: toward assisted fertilization by sperm-carrying micromotors. *Nano Lett.* 16:555–61
126. Edwards MR, Carlsen RW, Zhuang J, Sitti M. 2014. Swimming characterization of *Serratia marcescens* for bio-hybrid micro-robotics. *J. Micro-Bio Robot.* 9:47–60
127. Zhuang J, Sitti M. 2016. Chemotaxis of bio-hybrid multiple bacteria-driven microswimmers. *Sci. Rep.* 6:32135
128. Suh S, Traore MA, Behkam B. 2016. Bacterial chemotaxis-enabled autonomous sorting of nanoparticles of comparable sizes. *Lab Chip* 16:1254–60
129. Zhuang J, Carlsen RW, Sitti M. 2015. pH-taxis of biohybrid microsystems. *Sci. Rep.* 5:11403
130. Arabagi V, Behkam B, Cheung E, Sitti M. 2011. Modeling of stochastic motion of bacteria propelled spherical microbeads. *J. Appl. Phys.* 109:114702
131. Zhuang J, Wei G, Carlsen RW, Edwards MR, Marculescu R, et al. 2014. Analytical modeling and experimental characterization of chemotaxis in *Serratia marcescens*. *Phys. Rev. E* 89:052704
132. Cho S, Choi YJ, Zheng S, Han J, Ko SY, et al. 2015. Modeling of chemotactic steering of bacteria-based microrobot using a population-scale approach. *Biomicrofluidics* 9:054116
133. Zhuang J, Park BW, Sitti M. 2017. Propulsion and chemotaxis in bacteria-driven microswimmers. *Adv. Sci.* 4:1700109
134. Park SJ, Park S-H, Cho S, Kim D-M, Lee Y, et al. 2013. New paradigm for tumor theranostic methodology using bacteria-based microrobot. *Sci. Rep.* 3:3394
135. Karmakar R, Uday Bhaskar RVS, Jesudasan RE, Tirumkudulu MS, Venkatesh KV. 2016. Enhancement of swimming speed leads to a more-efficient chemotactic response to repellent. *Appl. Environ. Microbiol.* 82:1205–14
136. Tran T-H, Kim DH, Kim J, Kim MJ, Byun D. 2011. Use of an AC electric field in galvanotactic on/off switching of the motion of a microstructure blotted by *Serratia marcescens*. *Appl. Phys. Lett.* 99:063702
137. Wu Z, Li T, Li J, Gao W, Xu T, et al. 2014. Turning erythrocytes into functional micromotors. *ACS Nano* 8:12041–48
138. Erkoc P, Yasa IC, Ceylan H, Yasa O, Alapan Y, Sitti M. 2019. Mobile microrobots for active therapeutic delivery. *Adv. Ther.* 2:1800064
139. Akin D, Sturgis J, Ragheb K, Sherman D, Burkholder K, et al. 2007. Bacteria-mediated delivery of nanoparticles and cargo into cells. *Nat. Nanotechnol.* 2:441–49
140. Basel MT, Balivada S, Wang H, Shrestha TB, Seo GM, et al. 2012. Cell-delivered magnetic nanoparticles caused hyperthermia-mediated increased survival in a murine pancreatic cancer model. *Int. J. Nanomed.* 7:297–306
141. Ceylan H, Giltinan J, Kozielski K, Sitti M. 2017. Mobile microrobots for bioengineering applications. *Lab Chip* 17:1705–24
142. Stanton MM, Sánchez S. 2017. Pushing bacterial biohybrids to in vivo applications. *Trends Biotechnol.* 35:910–13
143. Medina-Sánchez M, Schmidt OG. 2017. Medical microbots need better imaging and control. *Nat. News* 545:406–8
144. Vilela D, Cossío U, Parmar J, Gómez-Vallejo V, Martínez A, et al. 2018. Medical imaging for the tracking of micromotors. *ACS Nano* 12:1220–27
145. Chan CTY, Lee JW, Cameron DE, Bashor CJ, Collins JJ. 2015. 'Deadman' and 'Passcode' microbial kill switches for bacterial containment. *Nat. Chem. Biol.* 12:82–86